

Article

Solid-to-Liquid Ratio Influenced on Adhesion Strength of Metakaolin Geopolymer Coating Paste Added Photocatalyst Materials

Liyana Jamaludin ^{1,2,*}, Rafiza Abd Razak ^{1,3}, Mohd Mustafa Al Bakri Abdullah ^{1,4,*}, Petrica Vizureanu ^{5,6,*}, Andrei Victor Sandu ^{5,7,8}, Shayfull Zamree Abd Rahim ² and Romisuhani Ahmad ^{1,2}

- ¹ Centre of Excellence Geopolymer and Green Technology (CEGeoGTech), Universiti Malaysia Perlis (UniMAP), Perlis 02600, Malaysia
 - ² Faculty of Mechanical Engineering & Technology, Universiti Malaysia Perlis (UniMAP), Perlis 01000, Malaysia
 - ³ Faculty of Civil Engineering & Technology, Universiti Malaysia Perlis (UniMAP), Perlis 01000, Malaysia
 - ⁴ Faculty of Chemical Engineering & Technology, Universiti Malaysia Perlis (UniMAP), Perlis 02600, Malaysia
 - ⁵ Faculty of Materials Science and Engineering, Gheorghe Asachi Technical University of Iasi, 700050 Iasi, Romania
 - ⁶ Materials Science and Engineering Section, Technical Sciences Academy of Romania, 030167 Bucharest, Romania
 - ⁷ Department of Research, Development and Innovation, Romanian Inventors Forum, 700089 Iasi, Romania
 - ⁸ National Institute for Research and Development for Environmental Protection INCDFM, 060031 Bucharest, Romania
- * Correspondence: liyanajamaludin@unimap.edu.my (L.J.); mustafa_albakri@unimap.edu.my (M.M.A.B.A.); peviz2002@yahoo.com (P.V.)

Abstract: Coating materials are used on surfaces such as steel and ceramic to offer protection, corrosion resistance, wear and erosion resistance, a thermal barrier, or aesthetics. Although organic coating materials such as epoxy resins, silane, and acrylic are widely used, there are restrictions and drawbacks associated with their use, including the ease with which cracking, hazardous and harmful human health and environment, peeling, and deterioration occur. Organic matrices also have the capacity to release vapor pressure, which can lead to the delamination of coatings. Geopolymer coating materials offer an environmentally friendly solution to this concern to encourage sustainable growth. The simplicity with which geopolymers can be synthesized and their low emission of greenhouse gases such as CO₂, SO₂, and NO_x are advantages of geopolymers. The advent of geopolymer coatings with photocatalytic properties is advantageous for the decomposition of pollution and self-cleaning properties. The aim of this paper is to study the optimum solid-to-liquid ratio of metakaolin geopolymer paste added TiO₂ and ZnO by adhesion strength. Through iterative mixture optimization, we investigated the effects of different design parameters on the performance of a metakaolin-based geopolymer as a coating material. The assessed material was a metakaolin which was activated by an alkali activator (a mixture of sodium hydroxide and sodium silicate), with the addition of titanium dioxide and zinc oxide as photocatalyst substances. Varying proportions of solid-to-liquid ratio were tested to optimize the best mix proportion related to the coating application. Adhesion analyses of geopolymer coating paste were evaluated after 7 days. According to the findings, the optimal parameters for metakaolin geopolymer coating material are 0.6 solid-to-liquid ratios with the highest adhesion strength (19 MPa) that is suitable as coating material and enhanced the properties of geopolymer.

Keywords: solid-to-liquid ratio; metakaolin; geopolymer; adhesion; coating; photocatalyst material



Citation: Jamaludin, L.; Razak, R.A.; Al Bakri Abdullah, M.M.; Vizureanu, P.; Sandu, A.V.; Abd Rahim, S.Z.; Ahmad, R. Solid-to-Liquid Ratio Influenced on Adhesion Strength of Metakaolin Geopolymer Coating Paste Added Photocatalyst Materials. *Coatings* **2023**, *13*, 236. <https://doi.org/10.3390/coatings13020236>

Academic Editors: Maria Bignozzi and Alexandru Enesca

Received: 12 December 2022

Revised: 15 January 2023

Accepted: 16 January 2023

Published: 19 January 2023



Copyright: © 2023 by the authors. Licensee MDPI, Basel, Switzerland. This article is an open access article distributed under the terms and conditions of the Creative Commons Attribution (CC BY) license (<https://creativecommons.org/licenses/by/4.0/>).

1. Introduction

Geopolymer materials generated by the interaction of an inorganic substance with an alkaline activator have impressive fire resistance, the ability to encapsulate hazardous waste, and are affordable; nevertheless, further study is required to fully exploit their use as a coating material. In addition, since it utilizes minerals of geological origin, the process is green and environmentally safe. The combination of geopolymers and

photocatalysts materials such as titanium dioxide and zinc oxide has been utilized to generate excellent coatings for buildings in the construction sector due to their aesthetic appearance and economical cleaning maintenance costs [1–3]. Photocatalyst materials are innovative materials that have emerged in recent years and are now being utilized to enhance the mechanical strength of cementitious materials as well as to improve their overall properties [4]. Utilizing geopolymers is one technique to minimize waste, particularly industrial waste, and investigate creative waste management strategies [5]. Geopolymers are beneficial due to their simplicity of synthesis and low emissions of greenhouse gases like CO₂, SO₂, and NO_x [6,7].

Geopolymerization is an innovative process that can transform many aluminosilicate minerals into geopolymers, which are useful products. Geopolymerization is a heterogeneous chemical reaction involving solid aluminosilicate oxides and alkali metal silicate solutions under very alkaline conditions and low temperatures that produce amorphous to semicrystalline polymeric structures composed of Si–O–Al and Si–O–Si links [8,9]. The activator is chosen and the type of material has the greatest impact on the geopolymerization activity [10–17]. This implies the activation of either material, geological, or industrial origin in the form of by-products, as a precursor that is abundant in alumina and silica [18–20]. The synthesis of geopolymer is classified into three primary stages. The first step involves the dissolving of aluminosilicate in a strong alkali solution. Next follows the reorientation of free ion clusters, and finally, polycondensation takes place. The geopolymerization process comprises an extremely quick chemical reaction that takes place in alkaline conditions with silicon and aluminum minerals. This reaction produces a three-dimensional polymeric chain and ring structure that is composed of bonds between silicon dioxide and aluminum oxide [21]. Numerous authors conducted in-depth research and monitoring of the geopolymerization reaction of metakaolin (MK). When exposed to an alkali solution, this amorphous form of metakaolin is believed to be very reactive. As a solid precursor, metakaolin, which is mostly made up of reactive silica and alumina, is utilized in the geopolymerization reaction, which is described in more detail as follows according to Yao et al. [22].

- i Dissolution steps: The Si–O–Si and Si–O–Al bonds of the minerals are segmented, which results in the formation of reactive precursors (Si(OH)₄ and Al(OH)₄) in the solution.
- ii Restructuring steps: The reactive aluminosilicate precursors have the characteristics of being mobile and thermodynamically stable before being gelled.
- iii Polycondensation steps: The polymerization of oligo-sialate molecules, which was then followed by their reticulation and the development of a network of polysialate with the three-dimensional framework.

As alkali activators to activate geopolymer, sodium hydroxide (NaOH) and sodium silicate (Na₂SiO₃) are utilized. Studies have demonstrated that the performance of geopolymer binders is dependent on a number of characteristics, including activator concentrations and solid-to-liquid ratios. Alkali activators facilitate the dissolution of reactive amorphous aluminosilicates for the polycondensation of oligomers and the formation of dense microstructures [23]. Na⁺ ions from NaOH are utilized to increase the dissolving rate and aid in the stability of silicate monomers and dimers in the solution [24]. The solid-to-liquid ratio (S/L) also affects the properties of geopolymer paste as a coating material. Guzman-Aponte et al. [25] examined the liquid/solid ratio (L/S), which was also manipulated at three different levels: 0.35 (dry consistency), 0.40 (medium consistency), and 0.45 (fluid consistency). The previous study shows that an increase in liquid content can speed up the dissolution of Al and Si precursor species, but it limits the polycondensation processes. Khan et al. [26] reported the compressive strength was raised from 30 MPa to 38 MPa as a result of the incorporation of nano-ZnO. It was discovered that the strength achieved its utmost potential when there was a critical concentration of nano-ZnO present at 0.5 wt.%. After 28 days, Nochaiya et al. [27] found that increasing the quantity of ZnO used as an additional material led to improvements in the compressive strength and physical attributes of concrete. According to

Garg et al. [28] the addition of ZnO into geopolymer paste will enhance the rate of reaction of sodium hydroxide-activated metakaolin and slow the rate of reaction.

The strength of the coating adhesion is one of the key characteristics that reveals the coating's overall quality. Interaction with the substrate requires that the geopolymer have strong adhesive properties in its capacity as a coating material. The second need for long-term durability is that the coating must retain its capacity to offer persistent adhesive during the coating's entire service life. Jiang et al. [29] studied the effect of geopolymer coating in concrete using fly ash combined with ground granulated blast-furnace slag, metakaolin, and Ordinary Portland cement added superplasticizer. The adhesive strength achieved between 1.5 to 3.4 MPa. Several factors affect the adhesive of coating between substrates, such as surface interactions, due to coatings that are liquid, have low surface tension, and have a low viscosity which improves wetting and capillary action. The impacts of the environment, such as exposure to moisture, light, heat, and pollutants, each play a factor in the gradual degradation of adhesion over the duration of time. According to Dilik et al. [30], the adhesive strength of medium-density fiberboard (MDF) samples covered with polyurethane-based paint was measured to be 3.62 MPa, which was reported to be the highest value but after being subjected to high levels of humidity, the surface texture of the MDF samples turned rougher. This served as a form of barrier between the coat and the substrate, hence lowering the adhesive strength of both. Basri et al. [31] optimized the rice husk-based geopolymer coating at S/L ratio 0.25 with an adhesion strength of 4.7 MPa. However, having a significant number of unreacted or partly reacted particles, may result in poor adhesion.

In this article, the performance of metakaolin geopolymer as a binder for coating material is examined. We studied the effect of the solid-to-liquid ratio (S/L) ratio on the adhesion strength of coated substrates at room temperature. This work was done to provide a suitable in situ application without high-temperature curing that is applicable to coatings with excellent adhesion strength. Our findings may encourage more research into the use of sustainable geopolymers in photocatalytic coatings.

2. Experimental Methods

2.1. Materials

Metakaolin is derived from kaolin clay and amorphous kaolinite is formed by heating kaolin between 500 °C and 800 °C. Metakaolin is classified as an aluminosilicate substance due to the varying quantities of alumina and silica. Metakaolin in this research was supplied by Kaolin (Perak, Malaysia) Sdn. Bhd. The chemical composition of metakaolin was determined using X-ray Fluorescent (XRF) spectrometer consists mainly SiO₂ (55%) and Al₂O₃ (38.3%) with a minor content of TiO₂ (2.48%) and Fe₂O₃ (1.53%). Figure 1 indicated the SEM images of metakaolin.

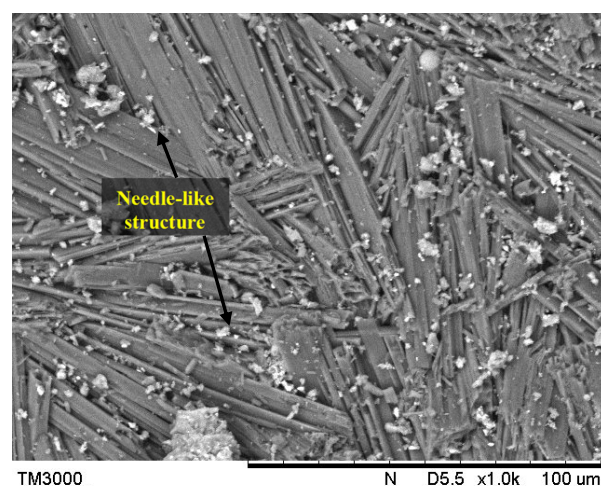


Figure 1. SEM images of metakaolin.

The alkali activator solution was prepared by mixing sodium hydroxide (NaOH) and sodium silicate (Na₂SiO₃) with mechanical stirrer for 5 min to obtain homogeneous solution. NaOH flakes with 98% purity obtained from AGC Chemicals (Bangkok, Thailand) Co., Ltd. was used to produce 10 M molarity by dissolving in a distilled water. Na₂SiO₃ supplied by PubChem has a specific gravity of 1.38 with liquid gel appearance. The alkaline solution was made 24 h prior to mixing before it was utilized to achieve a full exothermic reaction. This is to prevent the sudden setting of paste samples owing to the heat generated by hydration. Titanium dioxide (TiO₂) 98.0%–100% from Acros Organics (Geel, Belgium) was used in this study with density 4.23 g/cm³, and 79.88 g/mol molar mass. Zinc oxide from Sigma-Aldrich (Saint Louis, MS, USA), varied from 0.1 up to 0.9% chosen as photocatalyst material added in geopolymer paste.

2.2. Mix Design and Preparation of Metakaolin Geopolymer Paste

The solid-to-liquid (S/L) ratio varied throughout this analysis as shown in Table 1. The geopolymer paste (GP) was prepared by mixing metakaolin with Na₂SiO₃ and NaOH (alkaline activator solution) with overhead mechanical stirrer for 5 min until homogeneously. Alkali activator ratios were fixed at 2.5 and NaOH molarity at 10M based on previous research. Then, the GP was added with 5 wt.% of TiO₂ (GPTiO₂) and varying percentages of ZnO (0.1, 0.3, 0.5, 0.7 and 0.9 wt.%) by weight (GPTiO₂Zn). After prior mixing homogeneously, geopolymer paste was coated onto substrate by using brushing method. Mild steel plate was used as the substrate was cleaned with sandpaper to eliminate dirt and roughen the surface. The dimension of the mild steel substrate was 5.0 cm × 2.5 cm × 0.3 cm. Three layers of coating was applied to the substrate. After coating, the samples were cured at room temperature for 7 days. After 7 days of curing, the samples were tested with adhesion strength. The flow process has been summarized as Figure 2.

Table 1. Mix proportions of various S/L ratio of metakaolin geopolymer paste.

Mix	S/L	Metakaolin (g)	Alkali Activator (g)	TiO ₂ (wt.%)	ZnO (wt.%)
1	0.4	107	267.5	-	-
2	0.4	107	267.5	5	-
3	0.4	107	267.5	5	0.1
4	0.4	107	267.5	5	0.3
5	0.4	107	267.5	5	0.5
6	0.4	107	267.5	5	0.7
7	0.4	107	267.5	5	0.9
8	0.6	93.8	156.3	-	-
9	0.6	93.8	156.3	5	-
10	0.6	93.8	156.3	5	0.1
11	0.6	93.8	156.3	5	0.3
12	0.6	93.8	156.3	5	0.5
13	0.6	93.8	156.3	5	0.7
14	0.6	93.8	156.3	5	0.9
15	0.8	83.3	104.1	-	-
16	0.8	83.3	104.1	5	-
17	0.8	83.3	104.1	5	0.1
18	0.8	83.3	104.1	5	0.3
19	0.8	83.3	104.1	5	0.5
20	0.8	83.3	104.1	5	0.7
21	0.8	83.3	104.1	5	0.9

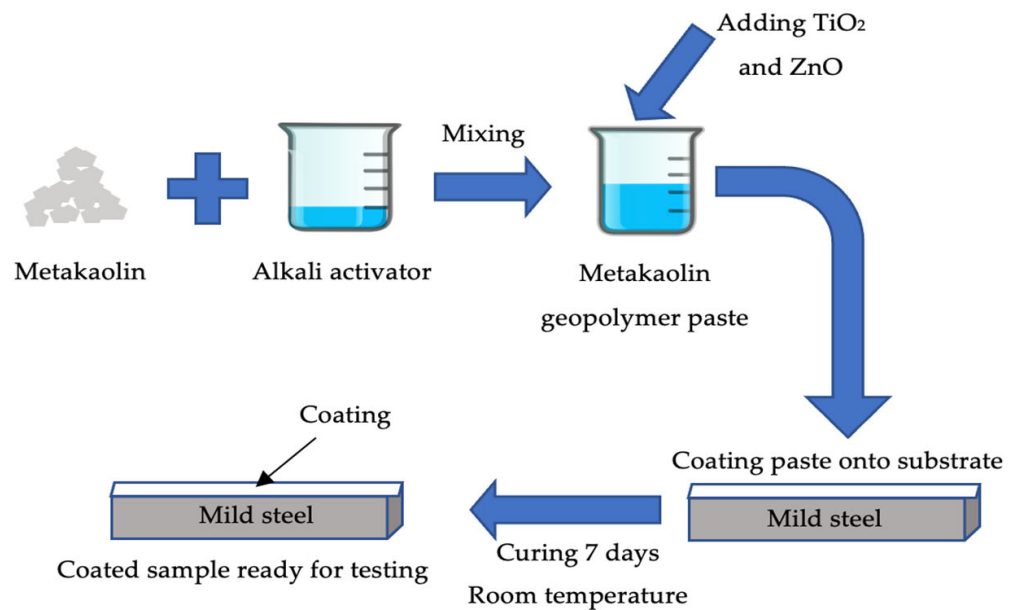


Figure 2. Schematic figure of flow process preparation of metakaolin geopolymer paste for coating.

2.3. Adhesion Strength Test

The most significance testing for coating is adhesion strength. The strength of metakaolin geopolymer paste added photocatalyst material was evaluated after 7 days of curing using Pull off Adhesion Tester brand Elcometer F106/3 from Elcometer Limited Company (Manchester, UK) according to ASTM D4541. A minimum of three samples were tested to evaluate the strength gain for the specimens. An adhesive was utilized to bond a test dolly to the metakaolin geopolymer layer for the adhesion procedure for 2 min. A pull-off adhesion test was utilized throughout the process to evaluate the level of cohesiveness that exists between the substrate and the coating. As the tension on the adhesion tester was increased, a spring system applied a lift force to the dolly. An indication on the scale depicts the numerical value of adhesion strength measured in terms of force per unit area. Figure 3 shows schematic diagram of the method of adhesion test occurs.

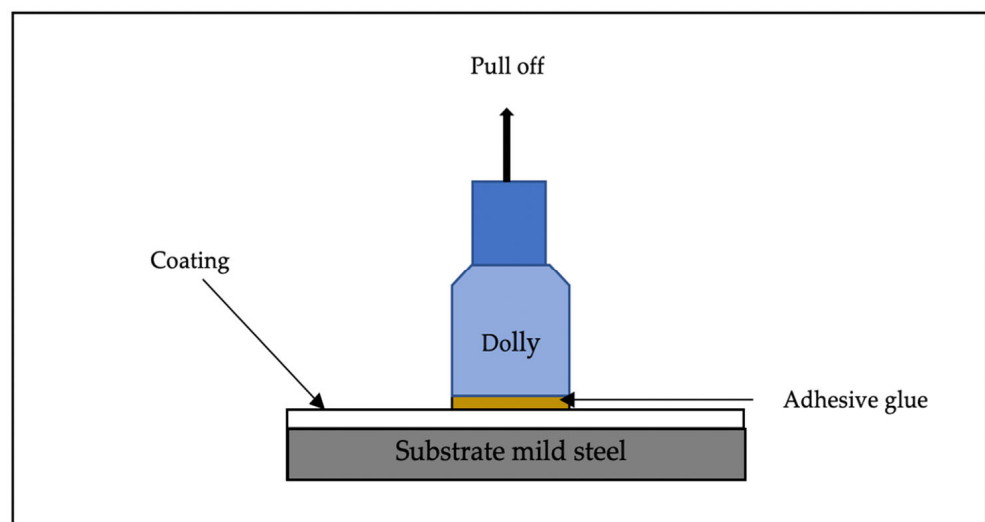


Figure 3. Schematic diagram of adhesion test.

2.4. Water Absorption and Density Test

The metakaolin geopolymer coating was tested for water absorption at 7 days of aging. The water absorption test was performed in accordance with ASTM D570-09 by immersing the samples in distilled water for 24 h. The samples were weighed, and their saturated weight was recorded after 24 h of immersion in distilled water. Equation (1) below specifies the water absorption calculation. Density was determined by weighing (W) and measuring the volume (V) of the samples using Densimeter MD-2003 (Qualitest, Plantations, FL, USA) to detect the specific gravity of the samples. The following Equation (2) was used to measure the density:

$$\text{Water absorption (\%)} = \{[\text{saturated weight} - \text{initial weight}]/\text{saturated weight}\} \times 100 \quad (1)$$

$$\text{Density (g/cm}^3\text{)} = \text{mass of sample}/\text{volume of sample} \quad (2)$$

2.5. Microscopic Test

Scanning electron microscopy: model TESCAN Vega, (Brno, Czech Republic) is used to analyze the microstructure properties of metakaolin geopolymer coating of each sample with acceleration voltage 20 kV. The energy dispersive spectroscopy (EDS) was performed on SEM images to identify the chemical compositions. For morphology of coating samples, the samples were cut into small pieces and the surface must be conductive before analyzing by coated with a gold monolayer of conductive substances. Auto Fine Coater Model JEOL JFC 1600 from Tokyo, Japan has been used for sputtering coater the samples with gold for conductivity.

3. Results and Discussion

3.1. Adhesion Strength Analysis

The adhesion strength was determined to identify the workability of metakaolin geopolymer paste for coating. The excellent adhesive strength of geopolymers is the basis for their application as substrate-interacting coating materials. Figure 4 shows the effect of S/L ratio based on adhesion strength between coating and substrate. The results indicate the optimum strength when S/L ratio is 0.6 before decreasing later due to faster setting time of the geopolymer paste at S/L ratio of 0.8. GPTiO₂Zn0.5 at S/L ratio 0.6 achieved the highest adhesion strength (19 MPa), while GPTiO₂Zn0.9 at S/L ratio 0.8 (2 MPa) drastically decreased the strength due to cracks occurring on the coating surface.

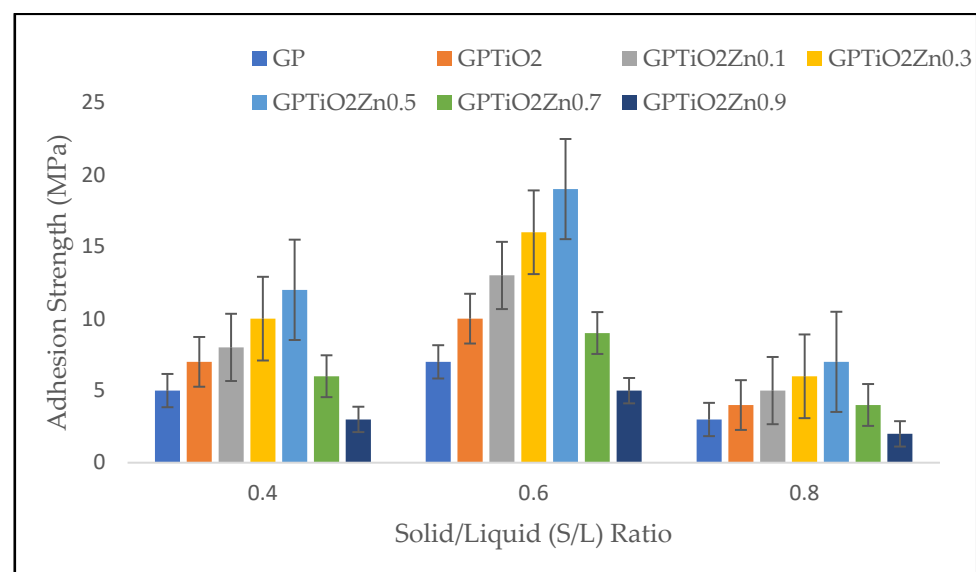


Figure 4. Adhesion strength of metakaolin geopolymer coating with various S/L ratios.

Figure 5 demonstrated the metakaolin geopolymer-coated sample with failure at S/L ratio of 0.6 for GP, GPTiO₂Zn0.5, and GPTiO₂Zn0.9. Coating samples with the highest and lowest adhesion strength together with GP as control sample were analyzed to learn which factors contributed to their respective performances.

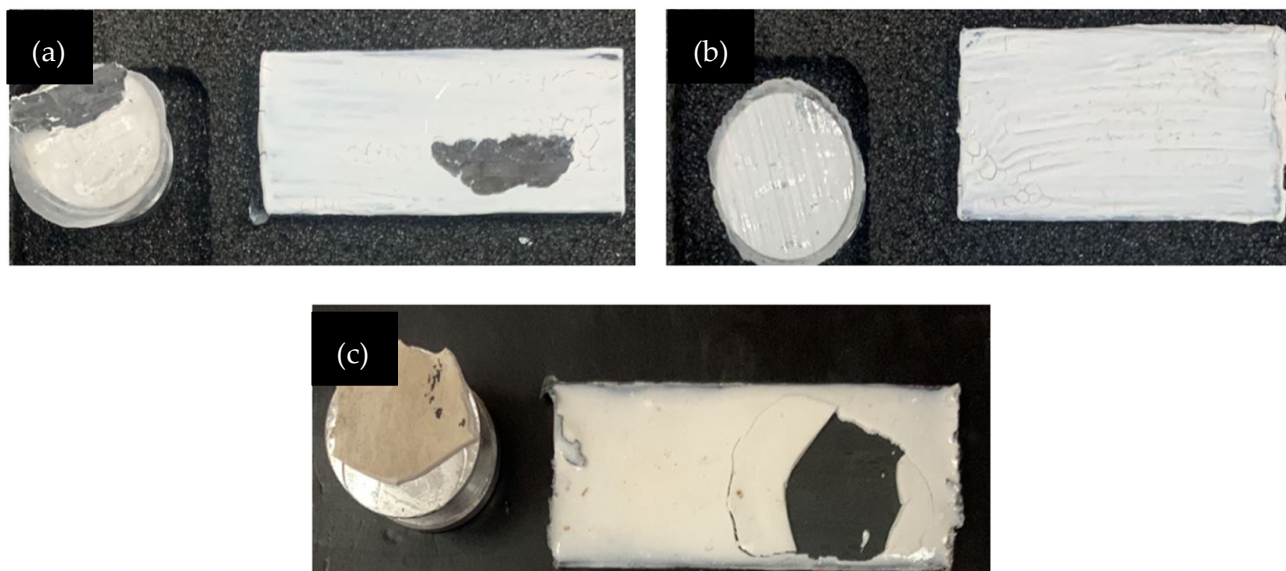


Figure 5. Adhesive failure on coating substrate (a) GP; (b) GPTiO₂Zn0.5; (c) GPTiO₂Zn0.9.

Based on its smaller particle size, metakaolin has considerably greater water consumption when compared to the other kind of geopolymer. This causes the workability of the metakaolin geopolymer paste to decrease when its S/L ratio is increased [23]. According to Ramasamy et al. [32], kaolin-based geopolymer specimens with a S/L ratio of less than 0.6 fail the curing stage due to the formation of major cracks. When ZnO 0.7 wt.% is added at various S/L ratios, the strength tends to decrease. The adhesion strength dropped when the ZnO doped was 0.7 and 0.9% because of agglomeration of nanoparticles that were not uniformly distributed throughout the material. However, by addition of TiO₂ and ZnO proof the cracks do not occur at S/L up to 0.6. ZnO is known as retarder in geopolymer system as if the amount of ZnO exceed more than 0.7 wt.%, it will affect the initial and final setting time [21]. Geopolymers containing ZnO demonstrated greater adhesion strength than unmodified geopolymer paste coating. This occurred because the interfacial adhesion that existed between the ZnO particles and the geopolymers resulted in the interfacial transition zone being reduced [33]. The data presented in the figure clearly showed adhesion strength improves as the amount of Si content and Na content increases. Poor adhesion was indicating at an S/L ratio of 0.8, which suggests that the amount of sodium hydroxide present plays an important role in the geopolymerization process. The adhesion strength first increases but subsequently declines as the ratio continues to increase.

Figure 6 indicates the schematic diagram of mechanism reaction between ZnO and geopolymer that contribute to enhancement in adhesion strength. Based on research by Wan et al. [34], through a combination of physical encapsulation and the adsorption of leached Zn²⁺ by geopolymer gel, zinc is enabled to become immobilized in the geopolymers. ZnO was partially dissolved in the leachate, and the geopolymers are responsible for the adsorption of the generated Zn²⁺. In charge-balancing sites inside the framework of geopolymer gel, Zn²⁺ partially replaced Na⁺ [21]. When the Ti and Zn filled the Na⁺, the voids on geopolymer structure will improve and increased the strength. The nucleation of the N-A-S-H gel is influenced by zinc and titanium interaction with phases involved in the alkali-activation process. The findings were relevant to the statement that the geopolymer has great ability for the adsorption of metal cations [35] which is related to the greater the formation of geopolymer gel, the higher number of cations absorbed. This resulting the

geopolymer exhibits a nucleation and filling effect, which contribute to the acceleration of the degree of reaction [25] when TiO_2 and ZnO have smaller particle size than the precursor and function as nucleation spots, hence facilitating the creation of reaction products [36].

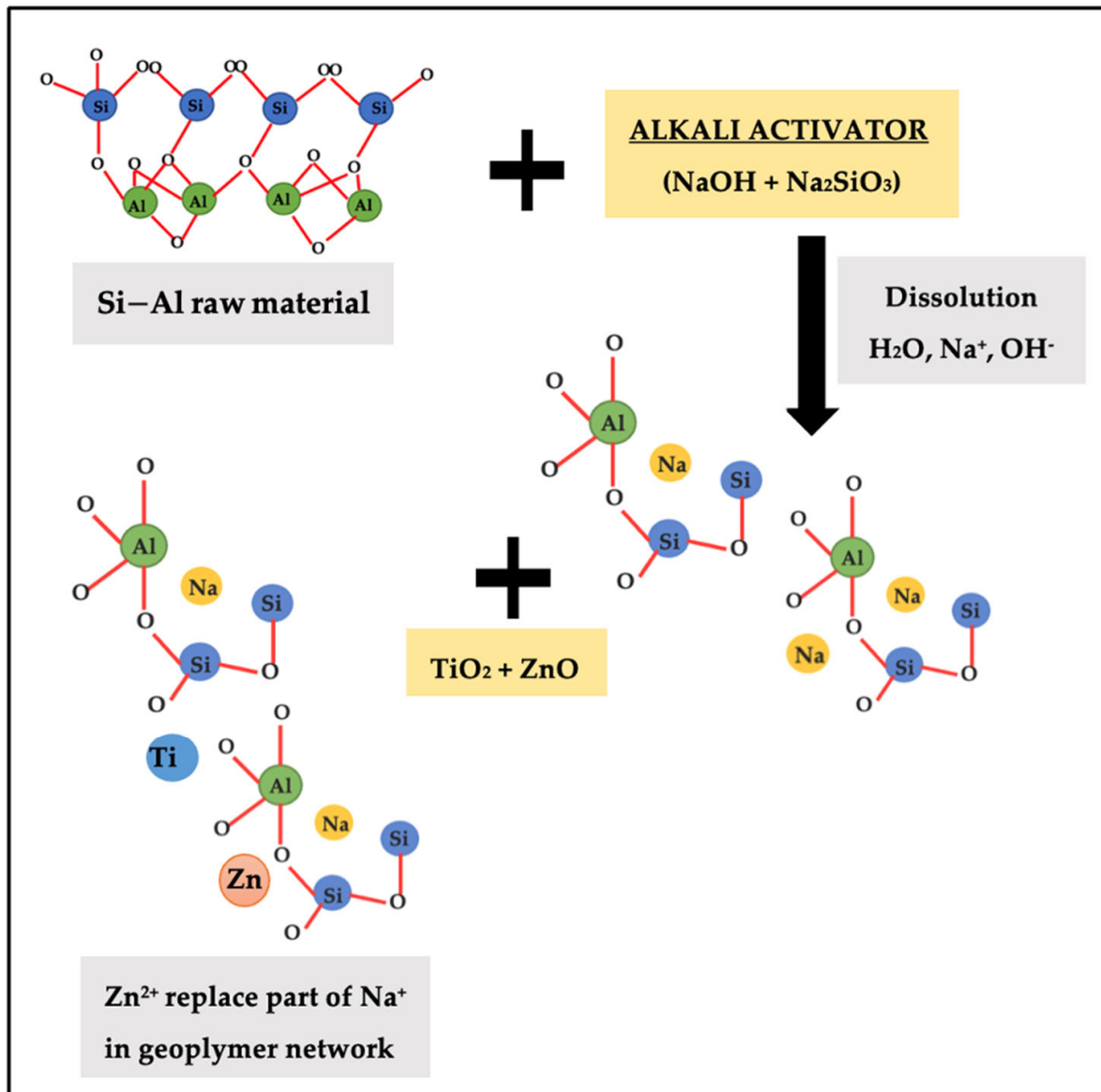


Figure 6. Schematic diagram of mechanism reaction between ZnO and geopolymer.

The usage of geopolymers as coating materials have a high adhesive strength, which allows them to function well with the substrate. Since the polymerization of a geopolymer happens extremely fast, geopolymers able to achieve a high strength during the early stages of their curing process [37,38]. Within seven days, the bonding strength of coatings reaches a maximum, then it remains constantly relevant with the previous statement from Khan et al. [26] stated the coatings may reach their greatest strength within the first 3 days of the curing process, and that the adhesion strength practically maintains the same even when the curing process is extended up to 180 days.

3.2. Microstructure Analysis

Figure 7 illustrates the microstructure of metakaolin geopolymer coating after 7 days of curing with an optimum S/L ratio of 0.6. These images show that geopolymerization products were formed in virtually all the samples despite the various amounts of ZnO and

addition of TiO_2 . Figure 7a shows geopolymer paste (GP) with several unreacted and half-reacted metakaolin with rough and uneven surfaces as indicated by the EDS test (Figure 8a). During the process of dissolving and polycondensing metakaolin, it was discovered that GP had unreacted metakaolin. This was caused by the fact that the metakaolin had not been dissolved by the alkaline activation conditions. This finding was in satisfactory correlation with research by Gutiérrez et al. [39]. Figure 7b indicates dispersion of TiO_2 and homogeneously reacted between MK and TiO_2 . Due to the filling effect, the inclusion of TiO_2 will increase the strength of the structure and decrease the porosity of the cement composites as reported by several researchers [40,41]. Incorporating ZnO into the geopolymer matrix led to an improvement in the homogeneity of the matrix with the increasing amount of ZnO which resulted in the network being denser and more compact as displayed in Figure 7c–g. According to the SEM, a homogeneous geopolymer matrix is produced when there is a high ratio of SiO_2 to Na_2O . This matrix becomes denser as the S/L ratio rises. This is caused that an increase in the S/L ratio will result in a denser gel structure, as well as a higher degree of dissolution and gel formation [42]. Wang et al. [43] and Alomayri et al. [44] stated because of the filling of voids in the microstructure, there is an interacted adhesion between the geopolymer matrix and the ZnO. It has been discovered that the incorporation of nanoparticles into geopolymer composites improves the strength of production of C-S-H gel and strengthens the interfacial transition zone [45]. It is conceivable that the Zn^{2+} cations contributed to the creation of a new gel phase and functioned in a way that was identical to that of Na^+ . Meanwhile, at 0.7–1.1 wt.% of ZnO added into the geopolymer matrix causes decreasing of adhesion strength. This phenomenon known as agglomeration of ZnO nanoparticles, which in turn, influences the formation of geopolymer gels by increasing the number of voids and, thus, decreasing the strength of the gels [46]. However, large portion of the activated raw materials which transformed into a dense gel matrix when ZnO added into the geopolymer due to the zinc is immobilized in the geopolymers through physical encapsulation and adsorption of the leached Zn^{2+} by geopolymer gel to form dense structure.

Figure 8a illustrates the EDS spot analysis for metakaolin geopolymer coating (GP) which shows the samples present homogenous chemical compositions with main elements consisting of sodium (Na), aluminum (Al) and silicon (Si). From Figure 8b, it is noticeable that the geopolymer matrix comprises the Al, Na, and Si with the trace of doping Ti and Zn. This element mentions confirmed the formation of N-A-S-H aluminosilicate binder nucleation which is responsible for the high strength. Decreasing Na content was observed with the replacement of Ti and Zn. When the Ti and Zn filled the Na^+ , the voids on geopolymer structure will improve and increase the strength.

3.3. Water Absorption and Density Analysis

Table 2 represents the water absorption and density of metakaolin geopolymer paste coating without ZnO and with various amounts of ZnO at S/L 0.6. The results indicate that increasing the percentage of ZnO decreased the absorption of water into the geopolymer coating and increased the density. GP sample without the addition of TiO_2 and ZnO shows the highest percentage of water absorption (1.92%) while $\text{GPTiO}_2\text{Zn}0.9$ has the lowest percentage which is 0.76%. It was discovered that the percentage of water absorption ranged from 0.76% to 1.92%. According to the findings of the research that Deshmukh et al. [47] carried out, the mass of the samples taken from each different mix did not alter substantially. This is because TiO_2 and ZnO nanoparticles have microporous diameters, which are beneficial to the development of adsorption and separation processes suitable to statement reported by Mustapha et al. [48]. Additionally, the range percentage of water absorption for this study was in excellent condition since the water absorption rate was less than 5% as mentioned by Mohd Azhar et al. [49].

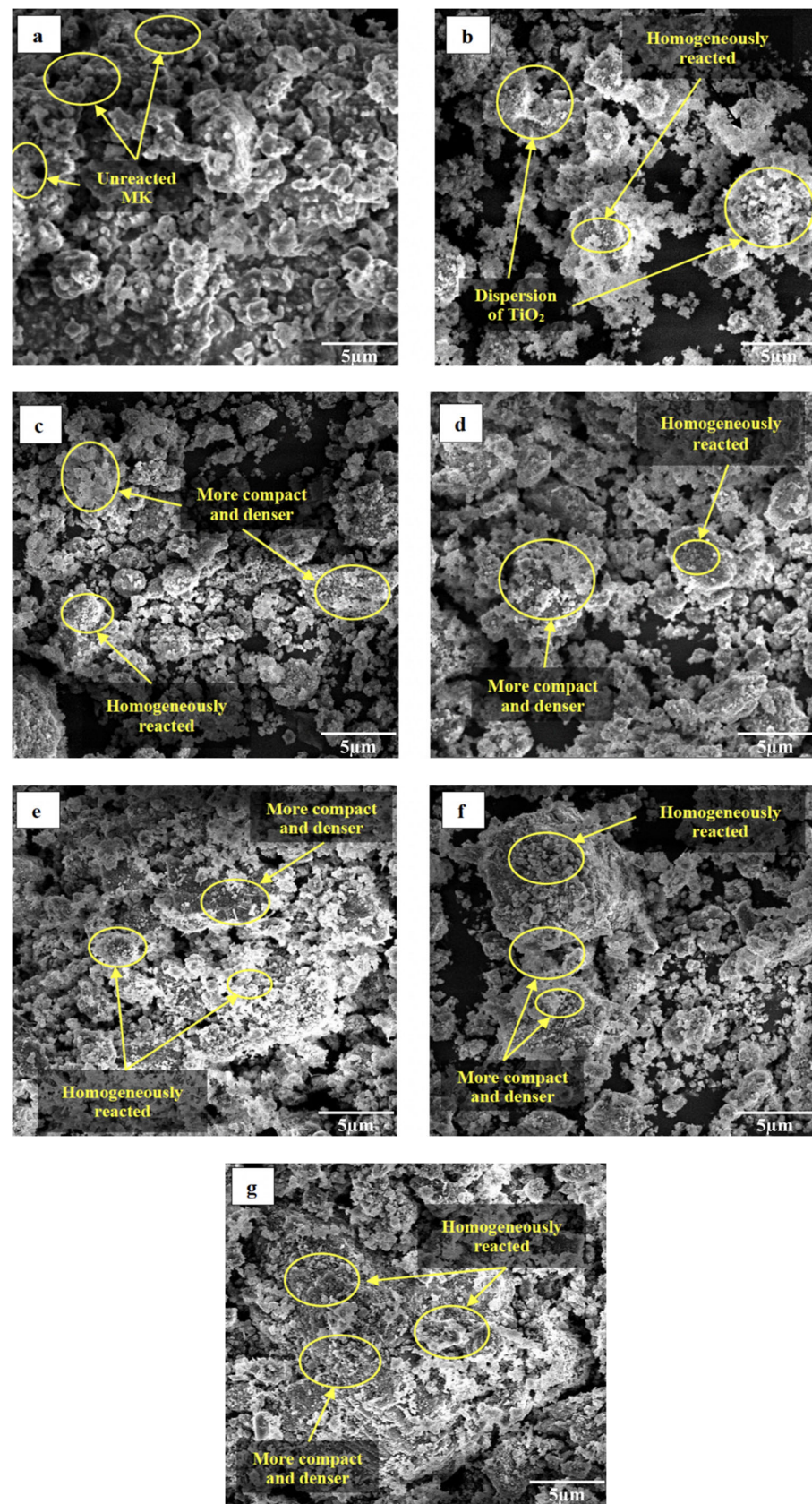
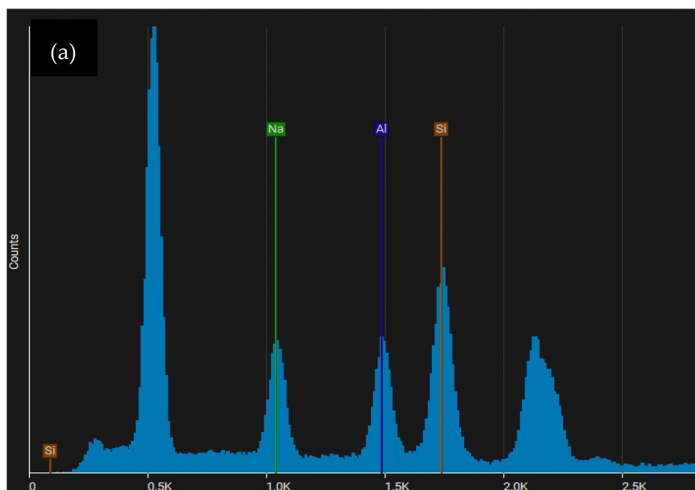
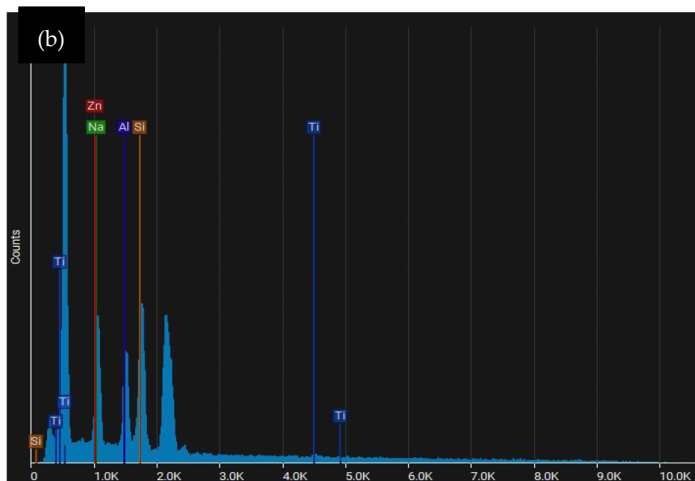


Figure 7. SEM images of metakaolin geopolymer coating: (a) GP; (b) GPTiO₂; (c) GPTiO₂Zn0.1; (d) GPTiO₂Zn0.3; (e) GPTiO₂Zn0.5; (f) GPTiO₂Zn0.7; (g) GPTiO₂Zn0.9.



Element	Atomic (%)	Weight (%)
Al	26.35	26.98
Si	45.4	48.38
Na	28.25	24.64



Element	Atomic (%)	Weight (%)
Al	24.78	21.63
Si	39.89	36.24
Na	20.09	14.95
Ti	8.91	13.8
Zn	6.32	13.38

Figure 8. EDS analysis of metakaolin geopolymer coating: (a) GP; (b) GPTiO₂Zn0.5.

Table 2. Water absorption and density analysis of metakaolin geopolymer coating at S/L ratio 0.6.

Mix	Water Absorption (%)	Density (g/cm ³)	Specific Gravity
GP	1.92	5.95	6.951
GPTiO ₂	1.74	6.17	6.919
GPTiO ₂ Zn0.1	1.58	8.26	6.420
GPTiO ₂ Zn0.3	1.17	8.17	7.129
GPTiO ₂ Zn0.5	1.1	7.45	7.345
GPTiO ₂ Zn0.7	1.12	7.46	7.346
GPTiO ₂ Zn0.9	0.76	7.99	7.055

The relationship between water absorption and density of metakaolin geopolymer coating is illustrated in Figure 9. The graph presented a clear illustration of an inverse correlation. As density from different mix designs increased, the water absorption from different mix designs decreased. As shown in SEM images previously, the decreased water absorption that occurs as a result of an increase in density is due to the microstructure geopolymer matrix being denser, more compact, and decrease in the number of pores. In addition, the incorporation of TiO₂ and ZnO into the geopolymer matrix helped to fill the small holes and enhance the microstructure of the material [50]. Zidi et al. [51] and Guzman et al. [25] reported similar findings that discovered the relationship between water absorption and density and found that the optimum ratio was GPTiO₂Zn0.5. Consequently,

this resulted in an improvement in both the water absorption and density of the metakaolin geopolymer coating [52]. The results demonstrated clearly that the addition of ZnO led to an improvement in the structural properties of geopolymers.

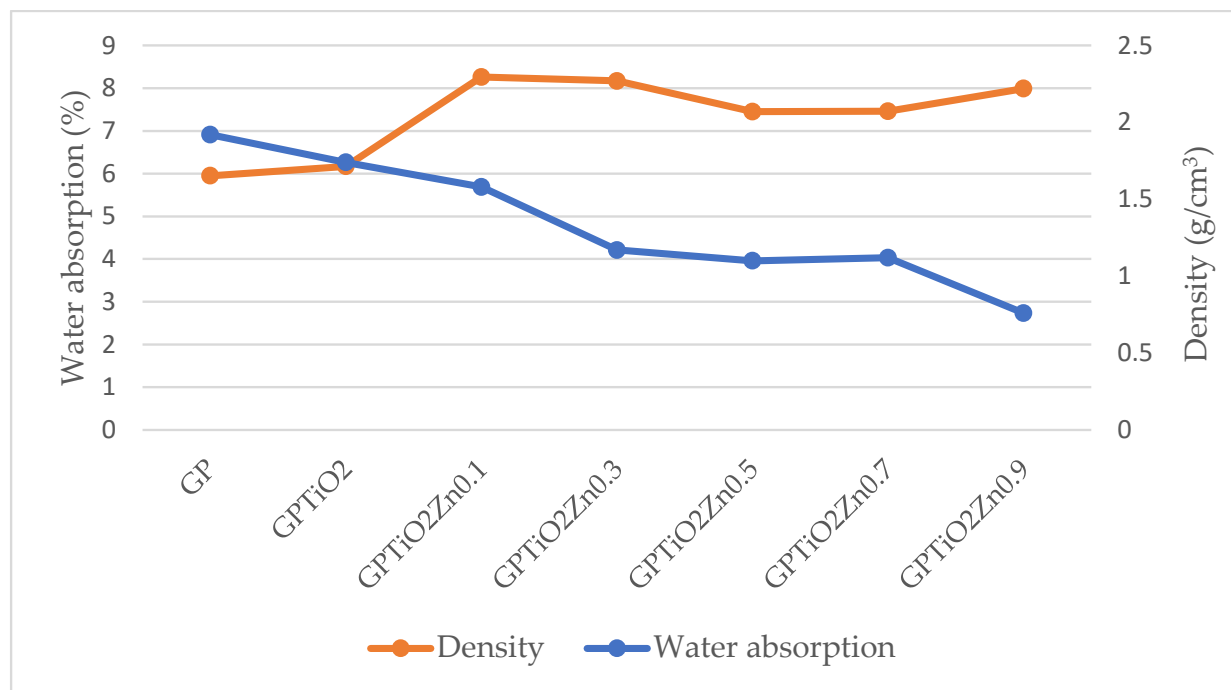


Figure 9. Water absorption versus density of metakaolin geopolymer coating paste.

4. Conclusions

According to the findings of the research that was carried out, the ratio of solid to liquid, together with the incorporation of photocatalyst components, plays a significant part in the capabilities of the metakaolin geopolymer coating in terms of adhesion strength, water absorption, and density. Metakaolin geopolymer coating paste contributed to the optimal S/L ratio of 0.6, as determined by the results of this investigation. The effects of adding TiO₂ and ZnO particles into the S/L ratio on metakaolin-based geopolymer were evaluated. The results indicate that the addition of titanium dioxide particles at fixed 5 wt.% and ZnO at up to 0.5 wt.% affect the formation of the N-A-S-H gel and these particles coexisted within it with the replacement of Na⁺. The nucleation of the N-A-S-H gel is influenced by zinc interaction with phases involved in the alkali-activation process. The maximum value of adhesion strength was achieved at 7 days of curing (19 MPa) at S/L 0.6 after the addition of 0.5 wt.% of Zn. However, the incorporation of 0.7 and 0.9 wt.% ZnO decreased the properties of the geopolymers. No improvement in the adhesion strength was found for materials with an S/L 0.8 due to cracks occurring on the surface.

The S/L ratio of metakaolin geopolymer paste and the percentage of photocatalyst materials added significantly impact the characteristics of metakaolin-based geopolymers. Between 0.6 and 0.8, the S/L ratio is associated with increased strength and decreased water absorption. It was discovered that the percentage of water absorption ranged from 0.76 to 1.92% excellent in coating properties as the water absorption is less than 5%. The microstructure of metakaolin geopolymer coating became denser and more compact after the addition of ZnO and TiO₂. The S/L ratio of less than 0.6 has a negative impact on porosity due to the formation of air bubbles. Due to the increased water consumption of metakaolin particles, a greater value of S/L decreases the workability. It is concluded that geopolymer with the addition of photocatalyst materials can be used as a green coating with high adhesion strength. Further studies, including self-cleaning characterization and pollutant degradation of coating, will be studied in the future.

Author Contributions: Conceptualization, L.J., R.A.R. and M.M.A.B.A.; data curation, L.J., R.A.R. and P.V.; formal analysis, L.J., R.A.R., R.A. and S.Z.A.R.; investigation, L.J., R.A.R., P.V., A.V.S., R.A. and S.Z.A.R.; methodology, L.J., R.A.R., M.M.A.B.A. and R.A.; project administration, R.A.R.; validation, R.A.R., P.V. and M.M.A.B.A.; writing of review and editing, L.J., R.A.R., A.V.S. and M.M.A.B.A.; All authors have read and agreed to the published version of the manuscript.

Funding: This study was supported by the Center of Excellence Geopolymer and Green Technology (CEGeoGTech) UniMAP and Gheorghe Asachi Technical University of Iasi (TUIASI) from the University Scientific Research Fund (FCSU).

Institutional Review Board Statement: Not applicable.

Informed Consent Statement: Not applicable.

Data Availability Statement: Not applicable.

Acknowledgments: The authors wish to extend their gratitude to the Center of Excellence Geopolymer and Green Technology (CEGeoGTech), Universiti Malaysia Perlis (UniMAP) and Gheorghe Asachi Technical University of Iasi for their support with providing all the necessary facilities.

Conflicts of Interest: The authors declare no conflict of interest.

References

1. Mahmed, N.; Nor Saffirah Zailan, S.; Mustafa Al-Bakri Abdullah, M. Influence of TiO₂ nanoparticles (wt%) onto the physical and mechanical properties of the TiO₂-geopolymer paste. *IOP Conf. Ser. Mater. Sci. Eng.* **2020**, *864*, 012177. [[CrossRef](#)]
2. Hamidi, F.; Aslani, F. TiO₂-based photocatalytic cementitious composites: Materials, properties, influential parameters, and assessment techniques. *Nanomaterials* **2019**, *9*, 1444. [[CrossRef](#)] [[PubMed](#)]
3. Andaloro, A.; Mazzucchelli, E.S.; Lucchini, A.; Pedferri, M.P. Photocatalytic self-cleaning coatings for building facade maintenance. Performance analysis through a case-study application. *J. Facade Des. Eng.* **2017**, *4*, 115–129. [[CrossRef](#)]
4. Jamaludin, L.; Razak, R.A.; Abdullah, M.M.A.B.; Vizureanu, P.; Bras, A.; Imjai, T.; Sandu, A.V.; Abd Rahim, S.Z.; Yong, H.C. The suitability of photocatalyst precursor materials in geopolymer coating applications: A review. *Coatings* **2022**, *12*, 1348. [[CrossRef](#)]
5. Vitola, L.; Pundiene, I.; Prankeviciene, J.; Bajare, D. The impact of the amount of water used in activation solution and the initial temperature of paste on the rheological behaviour and structural evolution of metakaolin-based geopolymer pastes. *Sustainability* **2020**, *12*, 8216. [[CrossRef](#)]
6. Petroche, D.M.; Ramirez, A.D. The environmental profile of clinker, cement, and concrete: A life cycle perspective study based on Ecuadorian data. *Buildings* **2022**, *12*, 311. [[CrossRef](#)]
7. Zhang, J.; Tian, B.; Wang, L.; Xing, M.; Lei, J. Mechanism of photocatalysis. In *Photocatalysis. Fundamentals, Materials and Applications*; Springer: Singapore, 2018.
8. Luhar, I.; Luhar, S. A comprehensive review on fly ash-based geopolymer. *J. Compos. Sci.* **2022**, *6*, 219. [[CrossRef](#)]
9. Kalaiyarrasi, A.R.R.; Partheeban, A.P. Influence of Si/Al ratio on the compressive strength of metakaolin based geopolymers. *Int. J. Earth Sci. Eng.* **2016**, *9*, 87–91.
10. Faris, M.A.; Abdullah, M.M.A.B.; Muniandy, R.; Ramasamy, S.; Hashim, M.F.A.; Junaedi, S.; Sandu, A.V.; Mohd Tahir, M.F. Review on mechanical properties of metakaolin geopolymer concrete by inclusion of steel fibers. *Arch. Metall. Mater.* **2022**, *67*, 261–267.
11. Burduhos Nergis, D.D.; Vizureanu, P.; Sandu, A.V.; Burduhos Nergis, D.P.; Bejinariu, C. XRD and TG-DTA study of new phosphate-based geopolymers with coal ash or metakaolin as aluminosilicate source and mine tailings addition. *Materials* **2021**, *15*, 202. [[CrossRef](#)]
12. Zailani, W.W.A.; Abdullah, M.M.A.B.; Arshad, M.F.; Razak, R.A.; Tahir, M.F.M.; Zainol, R.R.M.A.; Nabialek, M.; Sandu, A.V.; Wysłocki, J.J.; Błoch, K. Characterisation at the bonding zone between fly ash based geopolymer repair materials (GRM) and ordinary Portland cement concrete (OPCC). *Materials* **2020**, *14*, 56. [[CrossRef](#)] [[PubMed](#)]
13. Izzat, A.M.; Husin, K.; Abdullah, M.M.A.B.; Ghazali, C.M.R.; Tahir, M.F.M.; Sandu, A.V. Microstructural analysis of geopolymer and ordinary portland cement mortar exposed to sulfuric acid. *Mater. Plast.* **2013**, *50*, 171–174.
14. Azimi, E.A.; Abdullah, M.M.A.B.; Vizureanu, P.; Salleh, M.A.A.M.; Sandu, A.V.; Chaiprapa, J.; Yoriya, S.; Hussin, K.; Aziz, I.H. Strength development and elemental distribution of dolomite/fly ash geopolymer composite under elevated temperature. *Materials* **2020**, *13*, 1015. [[CrossRef](#)]
15. Burduhos Nergis, D.D.; Vizureanu, P.; Corbu, O. Synthesis and characteristics of local fly ash based geopolymers mixed with natural aggregates. *Rev. Chim.* **2019**, *70*, 1262–1267. [[CrossRef](#)]
16. Burduhos Nergis, D.D.; Abdullah, M.M.A.B.; Vizureanu, P.; Tahir, M.F.M. Geopolymers and their uses: Review. *IOP Conf. Ser. Mater. Sci. Eng.* **2018**, *374*, 012019. [[CrossRef](#)]
17. Shahedan, N.F.; Abdullah, M.M.A.B.; Mahmed, N.; Kusbiantoro, A.; Tammas-Williams, S.; Li, L.-Y.; Aziz, I.H.; Vizureanu, P.; Wysłocki, J.J.; Błoch, K.; et al. Properties of a new insulation material glass bubble in geopolymer concrete. *Materials* **2021**, *14*, 809. [[CrossRef](#)]
18. Bai, Y.; Guo, W.; Wang, X.; Pan, H.; Zhao, Q.; Wang, D. Utilization of municipal solid waste incineration fly ash with red mud-carbide slag for eco-friendly geopolymer preparation. *J. Clean. Prod.* **2022**, *340*, 130820. [[CrossRef](#)]

19. Luhar, S.; Luhar, I. Application of seawater and sea sand to develop geopolymer composites. *Int. J. Recent Technol. Eng. (IJRTE)* **2020**, *8*, 5625–5633. [[CrossRef](#)]
20. Azad, N.M.; Samarakoon, S.M.S.M.K. Utilization of industrial by-products/waste to manufacture geopolymer cement/concrete. *Sustainability* **2021**, *13*, 873. [[CrossRef](#)]
21. Wang, L.; Geddes, D.A.; Walkley, B.; Provis, J.L.; Mechtcherine, V.; Tsang, D.C.W. The role of zinc in metakaolin-based geopolymers. *Cem. Concr. Res.* **2020**, *136*, 106194. [[CrossRef](#)]
22. Yao, X.; Zhang, Z.; Zhu, H.; Chen, Y. Geopolymerization process of alkali–metakaolinite characterized by isothermal calorimetry. *Thermochim. Acta* **2009**, *493*, 49–54. [[CrossRef](#)]
23. Jindal, B.B.; Alomayri, T.; Hasan, A.; Kaze, C.R. Geopolymer concrete with metakaolin for sustainability: A comprehensive review on raw material's properties, synthesis, performance, and potential application. *Environ. Sci. Pollut. Res.* **2022**. [[CrossRef](#)]
24. Toniolo, N.; Rincón, A.; Avadhut, Y.S.; Hartmann, M.; Bernardo, E.; Boccaccini, A.R. Novel geopolymers incorporating red mud and waste glass cullet. *Mater. Lett.* **2018**, *219*, 152–154. [[CrossRef](#)]
25. Guzmán-Aponte, L.A.; de Gutiérrez, R.M.; Maury-Ramírez, A. Metakaolin-based geopolymer with added TiO₂ particles: Physicomechanical characteristics. *Coatings* **2017**, *7*, 233. [[CrossRef](#)]
26. Irfan Khan, M.; Azizli, K.; Sufian, S.; Man, Z. Sodium silicate-free geopolymers as coating materials: Effects of Na/Al and water/solid ratios on adhesion strength. *Ceram. Int.* **2015**, *41*, 2794–2805. [[CrossRef](#)]
27. Nochaiya, T.; Sekine, Y.; Choo-pun, S.; Chaipanich, A. Microstructure, characterizations, functionality and compressive strength of cement-based materials using zinc oxide nanoparticles as an additive. *J. Alloy. Compd* **2015**, *630*, 1–10. [[CrossRef](#)]
28. Garg, N.; White, C.E. Mechanism of zinc oxide retardation in alkali-activated materials: An in situ X-ray pair distribution function investigation. *J. Mater. Chem. A Mater.* **2017**, *5*, 11794–11804. [[CrossRef](#)]
29. Jiang, C.; Wang, A.; Bao, X.; Chen, Z.; Ni, T.; Wang, Z. Protective geopolymer coatings containing multi-componential precursors: Preparation and basic properties characterization. *Materials* **2020**, *13*, 3448. [[CrossRef](#)]
30. Dilik, T.; Erdinler, S.; Hazir, E.; Koç, H.; Hizirolu, S. Adhesion strength of wood based composites coated with cellulosic and polyurethane paints. *Adv. Mater. Sci. Eng.* **2015**, *2015*, 745675. [[CrossRef](#)]
31. Basri, M.S.M.; Mustapha, F.; Mazlan, N.; Ishak, M.R. Optimization of adhesion strength and microstructure properties by using response surface methodology in enhancing the rice husk ash-based geopolymer composite coating. *Polymers* **2020**, *12*, 2709. [[CrossRef](#)]
32. Ramasamy, S.; Hussin, K.; Abdullah, M.M.A.B.; Ghazali, C.M.R.; Binhussain, M.; Sandu, A.V. Interrelationship of kaolin, alkaline liquid ratio and strength of kaolin geopolymer. *IOP Conf. Ser. Mater. Sci. Eng.* **2016**, *133*, 012004. [[CrossRef](#)]
33. Gao, X.; Yu, Q.L.; Brouwers, H.J.H. Characterization of alkali activated slag–fly ash blends containing nano-silica. *Constr. Build. Mater.* **2015**, *98*, 397–406. [[CrossRef](#)]
34. Wan, Q.; Rao, F.; Song, S.; Zhang, Y. Immobilization forms of ZnO in the solidification/stabilization (S/S) of a zinc mine tailing through geopolymerization. *J. Mater. Res. Technol.* **2019**, *8*, 5728–5735. [[CrossRef](#)]
35. Kara, İ.; Yilmazer, D.; Akar, S.T. Metakaolin based geopolymer as an effective adsorbent for adsorption of zinc(II) and nickel(II) ions from aqueous solutions. *Appl. Clay Sci.* **2017**, *139*, 54–63. [[CrossRef](#)]
36. Essawy, A.A.; Abd, S. Physico-mechanical properties, potent adsorptive and photocatalytic efficacies of sulfate resisting cement blends containing micro silica and nano-TiO₂. *Constr. Build. Mater.* **2014**, *52*, 1–8. [[CrossRef](#)]
37. Rong, X.; Wang, Z.; Xing, X.; Zhao, L. Review on the adhesion of geopolymer coatings. *ACS Omega* **2021**, *6*, 5108–5112. [[CrossRef](#)]
38. Bhardwaj, P.; Gupta, R.; Mishra, D.; Sanghi, S.K.; Verma, S.; Amritphale, S.S. Corrosion and fire protective behavior of advanced phosphatic geopolymeric coating on mild steel substrate. *Silicon* **2020**, *12*, 487–500. [[CrossRef](#)]
39. De Gutiérrez, R.M.; Villalquira-Caicedo, M.; Ramirez-Benavides, S.; Astudillo, M.; Mejía, D. Evaluation of the antibacterial activity of a geopolymer mortar based on metakaolin supplemented with TiO₂ and CuO particles using glass waste as fine aggregate. *Coatings* **2020**, *10*, 157. [[CrossRef](#)]
40. Sorathiya, J.; Shah, S.; Smit Kacha, M.; Modhera, C.D.; Joshi, G.J.; Soni, D.; Patel, I.N.; Verma, A.K.; Zala, L.B.; Dhiman, S.D.; et al. Effect on addition of nano “titanium dioxide” (TiO₂) on compressive strength of cementitious concrete civil engineering. In Proceedings of the International Conference on Research and Innovations in Science, Engineering and Technology, Meerut, India, 26–27 August 2017; Volume 1.
41. Li, Z.; Han, B.; Yu, X.; Dong, S.; Zhang, L.; Dong, X.; Ou, J. Effect of nano-titanium dioxide on mechanical and electrical properties and microstructure of reactive powder concrete. *Mater. Res. Express.* **2017**, *4*, 095008. [[CrossRef](#)]
42. Rodríguez, E.D.; Bernal, S.A.; Provis, J.L.; Gehman, J.D.; Monzó, J.M.; Payá, J.; Borrachero, M.V. Geopolymers based on spent catalyst residue from a fluid catalytic cracking (FCC) process. *Fuel* **2013**, *109*, 493–502. [[CrossRef](#)]
43. Wang, J.; Du, P.; Zhou, Z.; Xu, D.; Xie, N.; Cheng, X. Effect of nano-silica on hydration, microstructure of alkali-activated slag. *Constr. Build. Mater.* **2019**, *220*, 110–118. [[CrossRef](#)]
44. Alomayri, T. Experimental study of the microstructural and mechanical properties of geopolymer paste with nano material (Al₂O₃). *J. Build. Eng.* **2019**, *25*, 100788. [[CrossRef](#)]
45. Barbhuiya, S.; Mukherjee, S.; Nikraz, H. Effects of nano-Al₂O₃ on early-age microstructural properties of cement paste. *Constr. Build. Mater.* **2014**, *52*, 189–193. [[CrossRef](#)]
46. Nivethitha, D.; Dharmar, S. Influence of zinc oxide nanoparticle on strength and durability of cement mortar. *Int. J. Earth Sci. Eng.* **2016**, *9*, 175–181.

47. Deshmukh, K.; Parsai, R.; Anshul, A.; Singh, A.; Bharadwaj, P.; Gupta, R.; Mishra, D.; Sitaram Amritphale, S. Studies on fly ash based geopolymeric material for coating on mild steel by paint brush technique. *Int. J. Adhes. Adhes.* **2017**, *75*, 139–144. [[CrossRef](#)]
48. Mustapha, S.; Ndamitso, M.M.; Abdulkareem, A.S.; Tijani, J.O.; Shuaib, D.T.; Ajala, A.O.; Mohammed, A.K. Application of TiO₂ and ZnO nanoparticles immobilized on clay in wastewater treatment: A review. *Appl. Water Sci.* **2020**, *10*, 49. [[CrossRef](#)]
49. Mohd Azhar, N.S.D.; Zainal, F.F.; Abdullah, M.M.A.B. Effect of different ratio of geopolymer paste based fly ash-metakaolin on compressive strength and water absorption. *IOP Conf. Ser. Mater. Sci. Eng.* **2019**, *701*, 012010. [[CrossRef](#)]
50. Ambikakumari Sanalkumar, K.U.; Yang, E.H. Self-cleaning performance of nano-TiO₂ modified metakaolin-based geopolymers. *Cem. Concr. Compos.* **2021**, *115*, 103847. [[CrossRef](#)]
51. Zidi, Z.; Ltifi, M.; ben Ayadi, Z.; Mir, L.E.L.; Nóvoa, X.R. Effect of nano-ZnO on mechanical and thermal properties of geopolymer. *J. Asian Ceram. Soc.* **2020**, *8*, 1–9. [[CrossRef](#)]
52. Paleu, C.C.; Munteanu, C.; Istrate, B.; Bhaumik, S.; Vizureanu, P.; Bălțatu, M.S.; Paleu, V. Microstructural analysis and tribological behavior of AMDRY 1371 (Mo–NiCrFeBSiC) atmospheric plasma spray deposited thin coatings. *Coatings* **2020**, *10*, 1186. [[CrossRef](#)]

Disclaimer/Publisher’s Note: The statements, opinions and data contained in all publications are solely those of the individual author(s) and contributor(s) and not of MDPI and/or the editor(s). MDPI and/or the editor(s) disclaim responsibility for any injury to people or property resulting from any ideas, methods, instructions or products referred to in the content.